International Journal of Advances in Scientific Research and Engineering (ijasre)

E-ISSN : 2454-8006

DOI: 10.31695/IJASRE.2023.9.7.1

Volume 9, Issue 7
July - 2023

Role of Formamidinium (FA) In the Electronic and Thermodynamic Properties of MA(Pb: Sn)I_3 Perovskites Using First Principle Calculations

Manala Tabu Mbumba[1*], Yujing Zhang[1], Yifan Yang[1], Muhammad Waleed Akram[1], Mina Guli[1]

[1] Beijing Key Laboratory of Novel Thin Film Solar Cells, New Energy School,

North China Electric Power University

Beijing, China

ABSTRACT

Research on perovskite solar cells employing tin to replace or partially replace lead is becoming more popular because of the recent achievement of about 24.2% conversion efficiency for ecologically benign mixed Pb-Sn perovskite solar cells. However, a smaller effect on cohesive energies caused by the addition of a Sn metal has a considerable effect on thermodynamic properties of Pb-Sn perovskites under high-temperature effects. This paper investigates the role of formamidinium in the electronic and thermodynamic properties of MA(Pb: Sn)I_3 perovskite alloy using density functional theory and CASTEP analysis through the Materials Studio. The intended A-cation perovskites have typical compounds FAx$MA_{1-x}Sn_{0.5}Pb_{0.5}I_3$, where x=0, 0.2, 0.4 and 0.6. The control and FA-based perovskites were computed through CASTEP analysis from Material studio to determine the electronic and thermodynamic properties. The findings revealed an improved thermodynamic properties of FA added perovskites compared to control ones whereby no significant effect was found in band gap of MAPb0.5Sn0.5I3 perovskite due to addition of formamidinium. However, when x is above 0.5, the quality of the perovskite films declined, with a wide grain size dispersion and little crystallization as well as the phase impurities were detected. This necessitated a theoretical approach to achieve an optimum amount of FA additive required to improve the properties as well as providing a theoretical guidance for improving the properties of perovskite materials before carrying out experiments. Furthermore, the study predicts that it is possible to create a stable thermal MA(Pb, Sn)I_3 alloy, if there is a well-thought-out design, which lays a foundation for the development and application of tin-lead mixed perovskite devices.

Keywords: Density Functional Theory, CASTEP software, Formamidinium, Pb-Sn Perovskite Solar Cells, Material studio, Thermodynamic property.

1. INTRODUCTION

Scientists' interest in the fast development of metal halide perovskites (MHP) as a cheap photovoltaic material has been sparked by the impending scarcity of electricity from conventional fossil fuels [1]. MHP based on lead iodide (PbI_2) and methylammonium (MA) has impressively achieved a 25.7% efficiency in lighting conversion devices [2,3] and a 24.2% [4] for a mixed Pb-Sn perovskite solar cells, laying the groundwork for future photovoltaic performance enhancements.

However, several issues remain, such as thermal instability, which necessitates a more profound knowledge of the chemical and structural properties associated with perovskite solar cell efficiency [5]. The thermal stability of the absorption layer has been improved by a variety of analyses carried out by researchers utilizing first-principles calculations [5]. Shi et al. [6] used generalized quasichemical approximation and density functional theory to perform first-principles calculations on the thermodynamic and ordering characteristics of $MAPb_{1-x}Si_xI_3$, $MAPb_{1-x}Ge_xI_3$, and $MAPb_{1-x}Sn_xI_3$ alloys as pseudo-cubic structures. The structural properties are significantly impacted by adding a second, more minor metal, such as Si or Ge, which decreases the organic cation's cavity volume and limits the free orientation under the influence of high temperatures. Density functional theory (DFT) was used by Zhou et al. [7] to examine how the T_e concentration affected the crystal structure, thermal stability, electronic structure, and optical properties of $Rb_2Sn_{1-x}Te_xI_6$ ($0 \leqslant x \leqslant 1$). The Sn-Te alloyed perovskites were found to have a good band gap, a small effective mass, and outstanding light absorption. Xia et al. [8] examined the electrical characteristics of the hybrid halide perovskite $(CH_2)_2NH_2PbI_3$ (AZPbI$_3$) using density functional theory (DFT); their findings have shown significant more stability than the widely used halide perovskites, i.e., $MAPbI_3$ and $HC(NH_2)_2PbI_3$. Additionally, they found that the Pb-Sn halides may have enhanced grain size and reduced trap-assisted nonradiative recombination, which would

have improved thermal stability [9-11]. Additionally, thermodynamic stability is essential to the viability of MHP-based solar cells for commercialization [10].

Recently, perovskites based on $MAPbI_3$ have opened up new possibilities for thermal stabilizing and tuning their properties in a variety of ways, including partial or total replacement of the MA^+ cation [11], [12]; Pb^{2+} atoms by another cation, such as Sn^{2+}; or varying the halogen content [13]. This method made significant progress in developing photovoltaic systems, particularly the $MAPb_{1-x}Sn_xI_3$ alloys, where the toxicity due to lead (Pb) is reduced by using another congener eco-friendly metal [14]. Based on this, the MHP alloys create space for the growth of photovoltaic performance by managing both their thermodynamic stability and optical qualities[15]. Experiment from previous research has revealed the thermodynamic stability of $MAPb_xSn_{1-x}I_3$ in distinct structural motifs over a relatively limited temperature range [16] and other weather variations like UV, heat, and moisture, which is critical for the durability of MHP solar cells [17]. Their result have revealed the tetragonal phase, which decomposes at temperatures as low as 403K, indicating that the alloy is thermodynamic unstable [18]. Recently, Hao et al. [19] investigated the $MAPb_xSn_{1-x}I_3$ stable alloy; their investigation revealed the pseudo-cubic structure for $MAPb_{0.5}Sn_{0.5}I_3$ alloy, but when the Pb content increases, the structure shifts to a tetragonal shape, indicating that the alloy is gradually approaching the stable thermal phase of $MAPbI_3$ [20]. Furthermore, with equal proportions of Pb: Sn the alloy is still found unstable at a temperature of 50℃, especially when its unencapsulated. This necessitates a theoretical study of perovskite alloys to determine the possibility of improving the thermal stability of mixed alloys.

To date, device architectures have been the main focus of most published solutions to perform outstanding thermal stability [21], [22]. Seo et al. [23] utilized new hole-transporting material with a fluorene termination to achieve 21 days of stability at 85°C in atmospheric condition. To address these shortcomings, research has focused on raising the perovskite layer's quality [11], [24]. The thermal stability of perovskite solar cells can be extended by increasing the activation energy for the perovskite film's thermal breakdown. However, by utilizing multiple distinct functional groups interacting with perovskite, there have been various attempts to make high-quality perovskites that address these issues. Dimethyl sulfoxide (DMSO) containing a S=O group was added by Park et al. [25] to inhibit the Lewis base-acid adduct technique of crystal formation. By generating fullerene-halide radicals, Wu et al. [26] used [6,6]-phenyl C61-butyric acid methyl ester (PCBM) to remove Pb-I defects. Several studies have also used comparable functional group small molecules or polymer additives in the volatile or non-volatile forms to suppress trap defects and enhance efficiency of the device [5], [27]. To increase thermal stability without abandoning its electrical capabilities, it is still challenging to control-oriented crystal formation and slow down crystal growth [28].

In this study, first-principle calculations through CASTEP analysis using Materials Studio were used to investigate the addition of formamidinium (FA) as a tactic to increase the properties of MA(Pb: Sn)I_3 perovskite [29], [30]. This strategy offers theoretical advice for enhancing the perovskite materials' characteristics through experimental means. The FA addition causes a stronger hydrogen bond to form, which causes the perovskite network to partially expand [31]. Additionally, FA promoted a favored orientation due to the increased activation energy. The perovskite films with FA had higher crystallinity, resulting in lower defect densities and better vertical charge transport, which were very efficient. However, excessive FA causes the film's quality to decline, with a wide grain size dispersion and little crystallization [32] and the phase impurities are detected when the FA addition exceeds 50% [33]. Hence a theoretical approach is also necessary to achieve an optimum amount of FA additive required to improve the properties.

2. METHODOLOGY

Both the control and the FA-added MA(Pb: Sn)I_3 perovskites were made using the DFT method and the CASTEP analysis from the Materials Studio simulation package [34]–[36]. The intended A-cation perovskites have typical compounds $FAxMA_{1-x}Sn_{0.5}Pb_{0.5}I_3$, where x=0, 0.2, 0.4 and 0.6 respectively. To generate the slab models, the Crystallography Open Database (COD) was used to extract the CIF files for FA and MA(Pb: Sn)I_3 [37]–[40]. FA was added to the MA(Pb: Sn)I_3 perovskite to produce the structures. The ultrasoft pseudopotential corresponding to a Perdew, Burke and Ernzerhof (PBE) exchange–correlation (XC) functional was employed. An energy cutoff of 500 eV, which have been adopted in the previous theoretical work in the similar systems, is employed and the atomic positions are optimized using XC functional until the maximum force less than 0.03 eV $Å^{-1}$ which was enough to obtain a relaxed structure [41]. The compounds were modeled with 4 × 3 × 4 Γ-centered grids for the k-point sampling. Tests were made for the 4 × 3 × 4 grid in the similar systems in previous theoretical work showing that the k-point grids are sufficient for the calculations [42]. The cell relaxing was carried out in accordance with the CASTEP analysis documentation [43]. The optical properties like dielectric functions, refractive index, absorption coefficient were calculated using the following formulas [35], [44].

DOI: 10.31695/IJASRE.2023.9.7.1

$$\varepsilon(\omega) = \varepsilon_1(\omega) + i\varepsilon_2(\omega) \quad (1)$$

$$\varepsilon_1(\omega) = 1 + \frac{2}{\pi} P \int_0^{\infty} \frac{\omega' \varepsilon_2(\omega')\partial\omega'}{(\omega'^2 - \omega^2)} \quad (2)$$

$$\varepsilon_2(\omega) = \frac{2\pi e^2}{\Omega\varepsilon_0} \sum_{k,v,c} |\Psi_k^c | u.r | \Psi_k^v|^2 \, \partial(E_k^c - E_k^v - E) \quad (3)$$

$$n(\omega) = \sqrt{\frac{\varepsilon_1(\omega)}{2} + \sqrt{\frac{(\varepsilon_1(\omega))^2 + (\varepsilon_2(\omega))^2}{2}}} \quad (4)$$

$$\alpha(\omega) = 2\omega \sqrt{\frac{-\varepsilon_1(\omega)}{2} + \sqrt{\frac{(\varepsilon_1(\omega))^2 + (\varepsilon_2(\omega))^2}{2}}} \quad (5)$$

$$E_{photon} = h.v = \frac{h.c}{\lambda} \quad (6)$$

$$V_{OC} = (nK_BT/q)\, ln\, (I/I_0 + 1) \quad (7)$$

Where ε_1 (ω) and ε_2 (ω)- the real and imaginary parts, ω - phonon frequency, P- the integral's principal value., e - electronic charge, Ω -the unit cell volume, u - the unit vector along the incident electric field's polarization, and Ψ_k^c and Ψ_k^v - conduction and valence band (VB) electrons' wave functions at a specific k, n- refractive index, α-absorption coefficient, E_{photon}- energy of the photon, h- Planck's constant, c- speed of light in vacuum, λ-frequency, I-light intensity, K_B - Boltzmann constant, T-temperature and q-elementary charge.

3. RESULTS & DISCUSSIONS

3.1 Electronic properties

The band gap is the energy range of a material where no feasible electronic state exists. It is the difference between the maximum valence and minimum conduction bands. Figure 1-4a demonstrates that the resultant band gap (E_g) has no discernible impact due to the addition of FA additive on $MAPb_{0.5}Sn_{0.5}I_3$ perovskite. The bandgap obtained was around 1.27 eV, which is comparable with previous findings which have shown the values from 1.2 to 1.3 eV [45], [46].

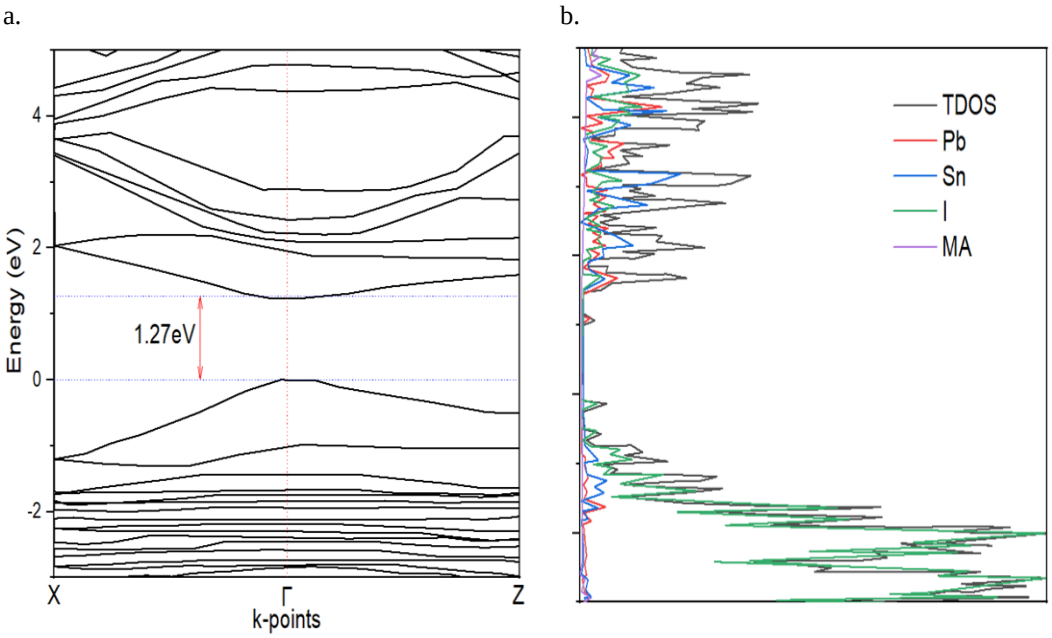

Figure 1. Band diagram and DOS of the control perovskite

DOI: 10.31695/IJASRE.2023.9.7.1

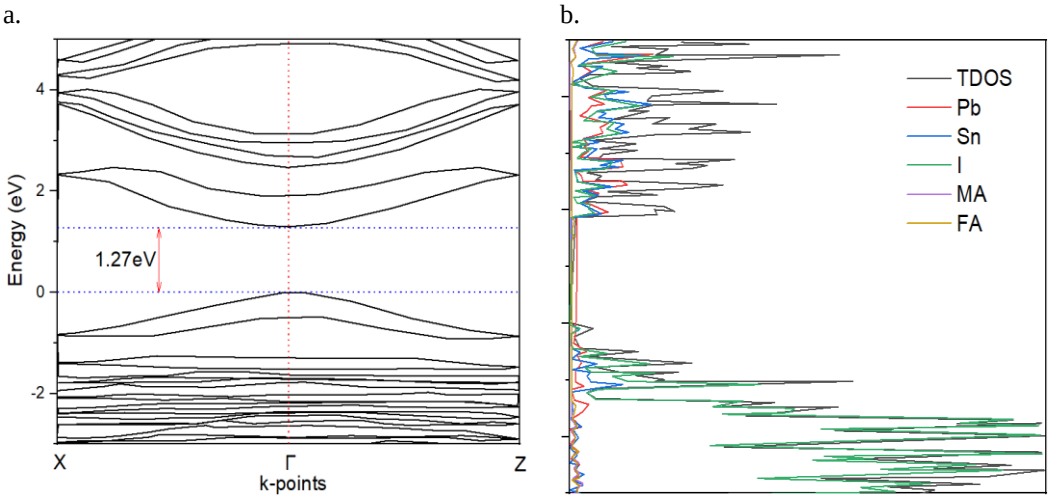

Figure 2. Band diagram and DOS of the $FA_{0.2}MA_{0.8}Pb_{0.5}Sn_{0.5}I_3$ perovskite

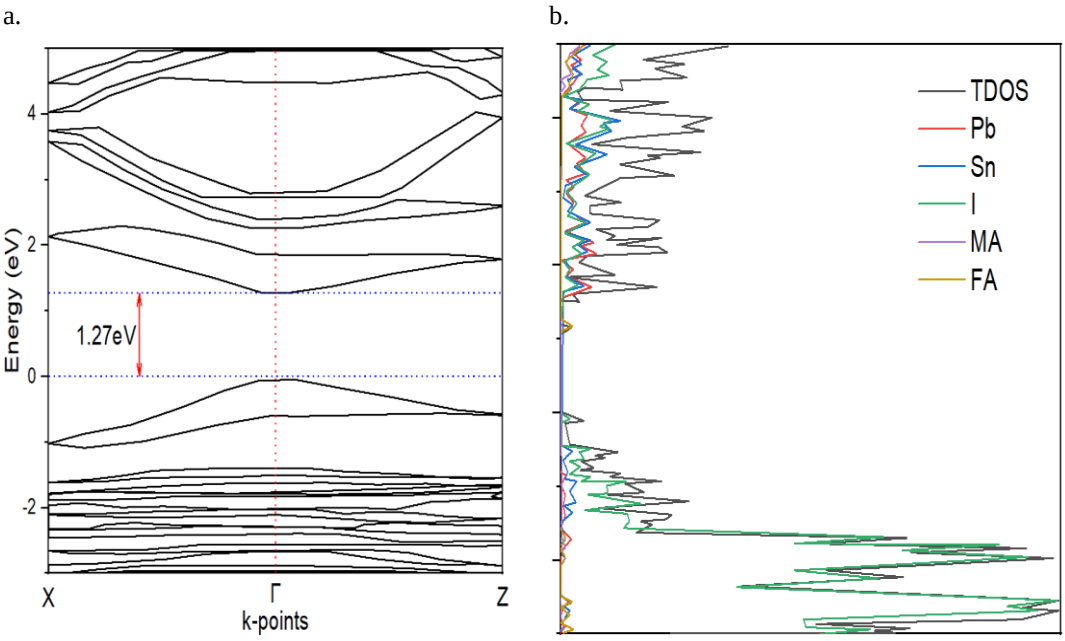

Figure 3. Band diagram and DOS of the $FA_{0.4}MA_{0.6}Pb_{0.5}Sn_{0.5}I_3$ perovskite

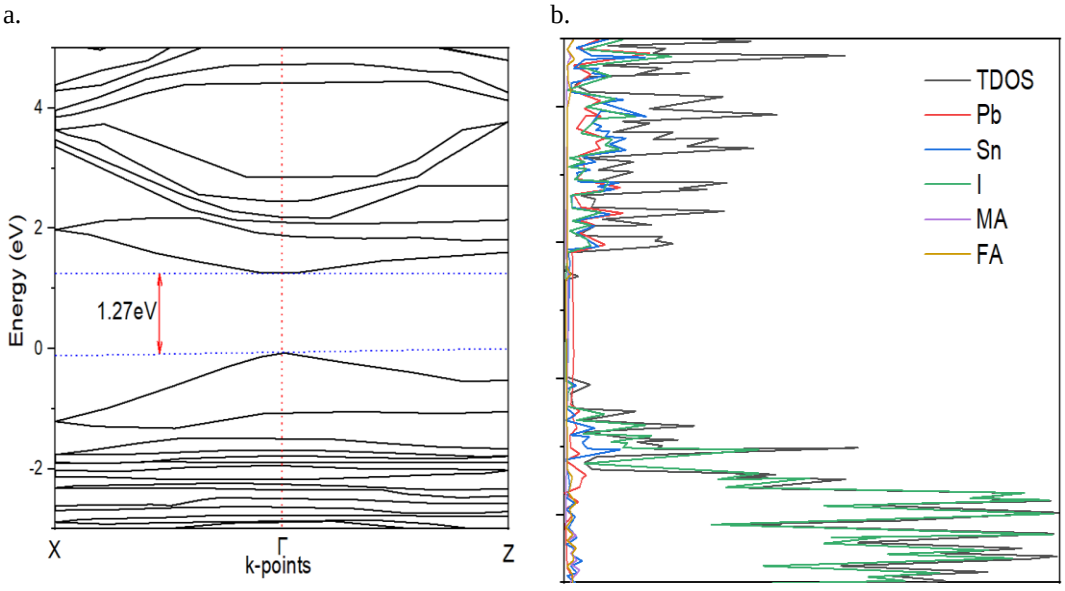

Figure 4. Band diagram and DOS of the $FA_{0.6}MA_{0.6}Pb_{0.5}Sn_{0.5}I_3$ perovskite

DOI: 10.31695/IJASRE.2023.9.7.1

Total Density of States (TDOS) measures the number of electronic states that exist in the material under consideration and have a specific energy. The GGA-PBE approximation was used to calculate the overall density of perovskite states, which is shown in Figures 1-4b. The TDOS profile displays the locations of distinctive peaks as well as the involvement of the FA, C, N, H, Pb, Sn, and I atoms' electronic states that interact to generate perovskites. The TDOS spectra displays the separate valence band-containing portions and the conduction band-containing region. The band gap is illustrated by the division between the lower region of the conduction states and the top portion of the valence states. This suggests that the hybrid perovskite structure behaves like a semiconductor.

3.3 Optical properties

Understanding the optical characteristics is an important topic that needs more research as the materials could be used as a light-harvesting medium. Understanding the dielectric function is crucial for understanding data on the charge-recombination rate and the efficiency of optoelectronic devices since a high dielectric constant enhances overall device performance and lowers charge carrier recombination [47]. The complex dielectric function ε (ω), which depicts a system's linear response to an external electromagnetic field, can be used to explain the optical properties of matter. The ability of a material to permanently absorb energy from an electric field is described by the imaginary part of the dielectric constant, whereas the real component of the dielectric constant describes the material's electronic polarizability. The static value of the dielectric constant of 20%–60% mol FA addition to the device at 0 eV is higher than that of the control device, and it started to decline when the ratio was above 50% because of phase impurities in the compound. This is revealed by the real part of the dielectric function, as shown in Figure 5. Consequently, the low energy region has a larger dielectric coefficient than the high energy region, which suggests that there is less charge-carrier recombination there, improving device performance in the visible spectrum.

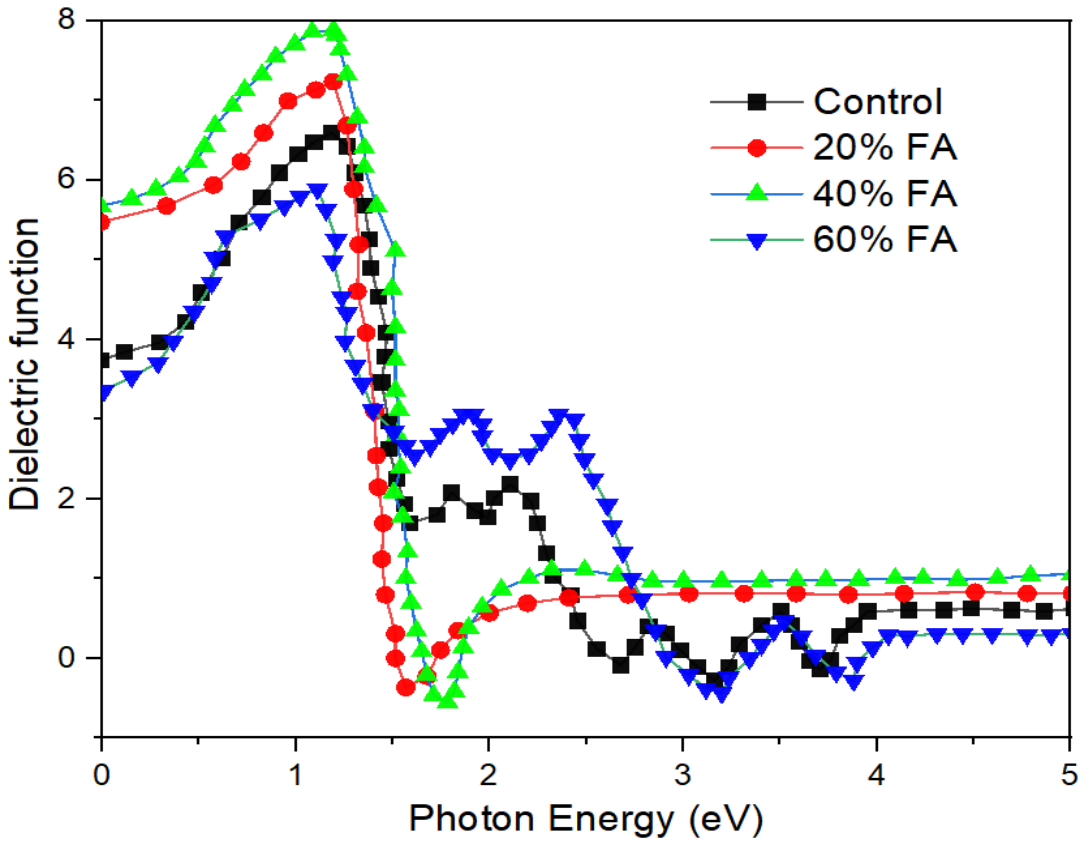

Figure 5. Real part of Dielectric function

Figure 6 provides a calculation of the imaginary portion of the dielectric function. Understanding the absorption behavior requires an understanding of the imaginary part, which is also associated with the band structure [44]. For both the control and the FA added devices, a strong peak in the visible region is seen. The 40% mol FA added device's peaks shifted more to the lower energy region revealing the strong absorption in the visible-range [48]. Similarly, the dielectric function of the FA added device is found to be minimal in comparison to the control device in the high-energy region. This implies low absorption in the higher energy region. Overall, the findings indicate that the FA-added device exhibits strong absorption in the low energy range, making it appropriate for use in optoelectronic applications like solar cells [49].

DOI: 10.31695/IJASRE.2023.9.7.1

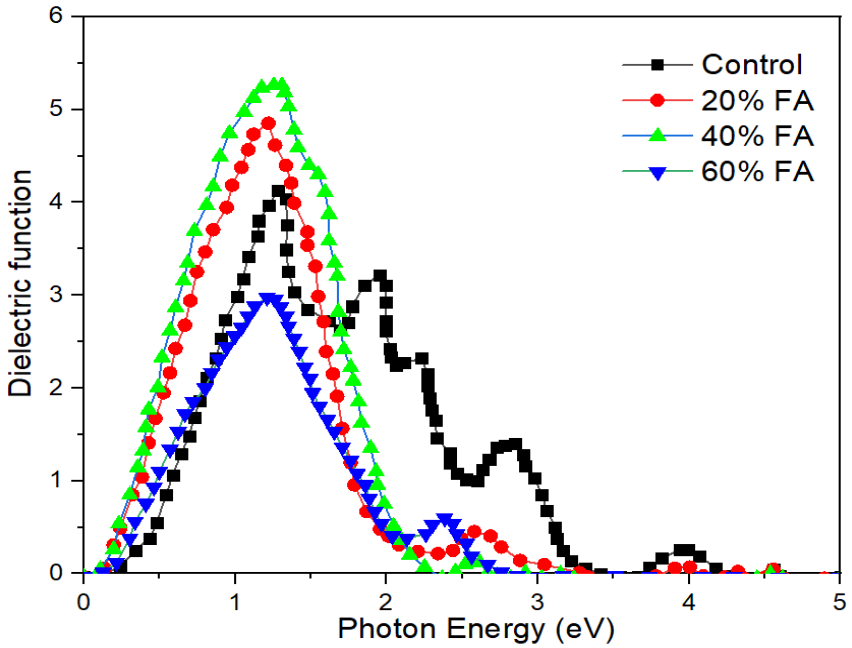

Figure 6. Imaginary part of Dielectric function

Another optical characteristic that was calculated in this study is the absorbance of the materials. This parameter provides additional, crucial details about the optimal solar energy conversion efficiency and the light entrance of a certain wavelength prior to absorption. The sun releases photons of light at various frequencies. The band gap width (Eg) of the materials is what determines whether a photon can be absorbed [50], meaning that if the photon's energy is lower than the band gap, it cannot be absorbed, and if it is equal to or higher than the band gap, it can be absorbed by the semiconductor [35]. Additionally, when the photon energy exceeds the band gap width, the bands relax toward the electronic states close to the gap, which results in energy loss. The addition of FA does not significantly affect the resulting Eg of the control as shown in Figure 7 instead the FA addition was responsible for lowering the crystallization rate which was caused by presence of 50%mol Sn in the control as a result the morphology of the material was poor due to their associated rapid crystallization [46].

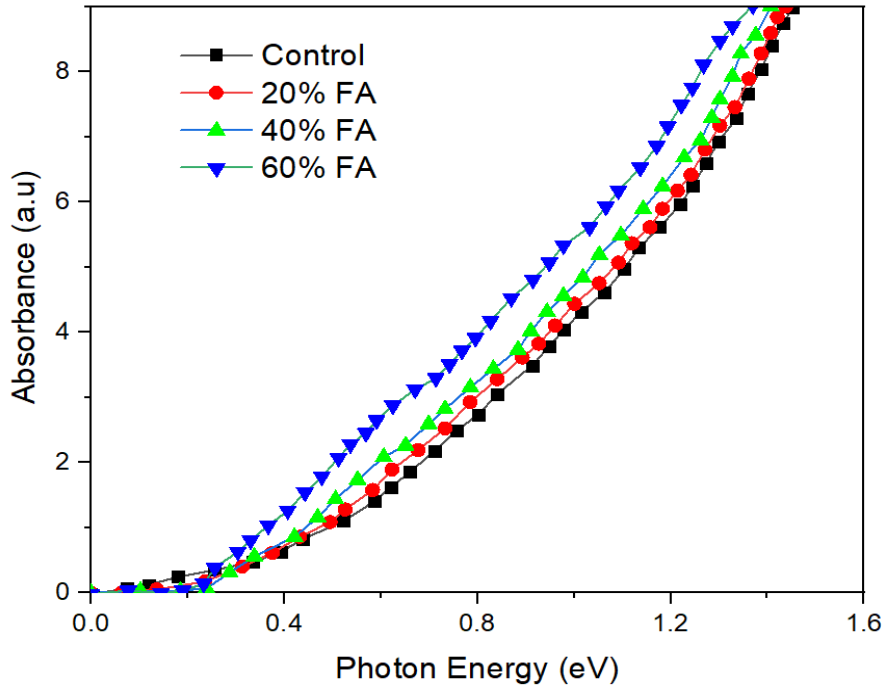

Figure 7. Calculated the absorption coefficient in the visible region

This study also took into account an optical conductivity, which provides a relationship between the amplitude of the inducing electric field and the current density produced in the material for arbitrary frequency [51]. The optical conductivity of perovskites is given in Figure 8 showing an improved photoconductivity of materials in the lower energy region. The greater absorption (Figure 7) in the visible area is the cause of the increased photoconductivity there. The samples' shape and peaks shifted toward

DOI: 10.31695/IJASRE.2023.9.7.1

the lower energy region. Compared to the control sample, the FA supplemented sample shifted more. The optical conductivity of the FA sample is therefore considerable throughout the entire visible light spectrum. This suggests that optimal FA addition would be more suited for usage in optoelectronic applications such as solar cells.

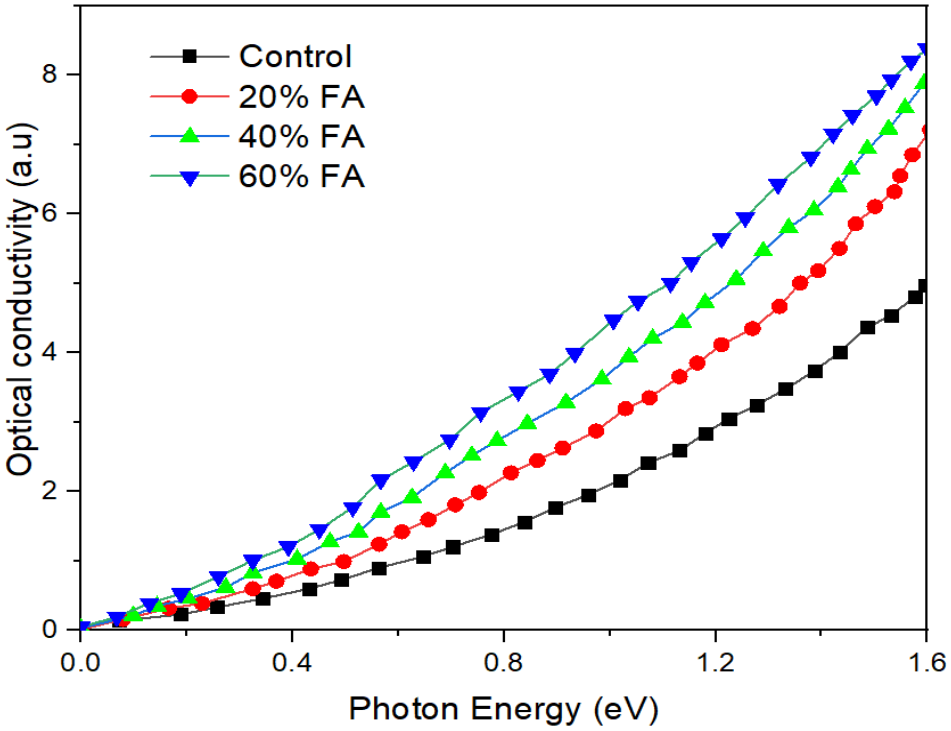

Figure 8. Calculated optical conductivity in the visible region

3.4 Thermodynamic properties

The stability of materials during moisture, light, and heat exposure is primarily determined by the energy of the breakdown reaction and the enthalpy of synthesis of the perovskite solar cell materials [5], [52]. Under the influence of high temperatures, tin and lead halide perovskites based on methylammonium quickly transform into the halides [53], [54].

The formation energies of the perovskites need be calculated to assess their thermodynamic properties. The overall formula for the perovskite formation process is MAI + PbI_2 → $MAPbI_3$, and the formation energy can be calculated as follows [55], [56].

$$\Delta H_f = E(MAPbI_3) - E(MAI) - E(PbI_2) \quad (8)$$

For the mixed perovskites $FA_xMA_{1-x}Sn_{0.5}Pb_{0.5}I_3$ perovskites, the formation energies (ΔH) are estimated by the following expression:

$$\Delta H_f = E(FA_xMA_{1-x}Sn_{0.5}Pb_{0.5}I_3) - [xE(FAI) + (1-x)E(MAI) + 0.5E(PbI_2) + 0.5E(SnI_2)] \quad (9)$$

Where x is the percentage of FA atoms, and ΔH_f is the enthalpy of formation for formula unit of $FAxMA_{1-x}Sn_{0.5}Pb_{0.5}I_3$. When ΔH is negative, the decomposition reactions become endothermic and indicates a perovskite structure is stable [56].

The formation energy per formula unit of $FAxMA_{1-x}Sn_{0.5}Pb_{0.5}I_3$ perovskites as listed in Table 1 reveals that; with the addition to 40% mol FA, the formation energies tend to decrease implying a more thermal stable structure than the control. This may be caused by the decrease in crystallization rate by presence of FA. When the FA level exceeds 50 mol%, the film morphology deteriorates once more, possibly as a result of phase impurities brought on by the perovskites' immiscibility [57], this led into the increase of energy. These results are comparable with the literature data for the Pb-Sn halide perovskite [55], [58]–[60].

Table 1. Formation energy (ΔH) per formula unit calculated using DFT/PBE functional

Crystal lattice	ΔH (eV)
Control	-4.43
20% FA	-5.6
40% FA	- 6.4
60% FA	-5.3

DOI: 10.31695/IJASRE.2023.9.7.1

4. CONCLUSIONS

FA additive was found to improve the properties of Pb-Sn perovskites. FA 's intense interaction with Pb/Sn ions boosted the film's growth activation energy, enabling the development of high-quality films with favored orientation and superior electrical characteristics. This predicts that it is possible to create a Pb.Sn alloy, if there is a well-thought-out design, which lays a foundation for the development and application of tin-lead mixed perovskite devices.

Conflict of Interest

There are no conflicts to declare.

REFERENCES

[1] J. Shamsi, A. S. Urban, M. Imran, L. De Trizio, and L. Manna, "Metal Halide Perovskite Nanocrystals: Synthesis, Post-Synthesis Modifications, and Their Optical Properties," *Chem. Rev.*, vol. 119, no. 5, pp. 3296–3348, 2019, doi: 10.1021/acs.chemrev.8b00644.

[2] H. Min, D.Y. Lee, J. Kim, G. Kim, K.S. Lee, J. Kim, M.J. Paik, Y.K. Kim, K.S. Kim, M.G. Kim, and T.J. Shin , "Perovskite solar cells with atomically coherent interlayers on SnO_2 electrodes," *Nature*, vol. 598, pp. 444–450, 2021, doi: doi.org/10.1038/s41586-021-03964-8.

[3] J.T. Matondo, M.D. Malouangou, J. Wu, L. Bai, Y. Yang, Y. Zhang, J. Pan, M. Cai, M.T. Mbumba, M.W. Akram, and Guli, M, "Lead acetate ($PbAc_2$)-derived and chloride-doped $MAPbI_3$ solar cells with high fill factor resulting from optimized charge transport and trap state properties," *Sol. Energy*, vol. 228, no. August, pp. 129–139, 2021, doi: 10.1016/j.solener.2021.09.010.

[4] J. Cao, H.L. Loi, Y. Xu, X. Guo, N. Wang, C.K. Liu, T. Wang, H. Cheng, Y. Zhu, M.G. Li, and W.Y. Wong, "High-performance tin-lead mixed perovskite solar cells with vertical compositional gradient," *Adv. Mater*, p. https://doi.org/10.1002/adma.202107729, 2021, doi: 10.1002/adma.202107729.

[5] M. T. Mbumba, D. M. Malouangou, J. M. Tsiba, L. Bai, Y. Yang, and M. Guli, "Degradation mechanism and addressing techniques of thermal instability in halide perovskite solar cells," *Sol. Energy*, vol. 230, no. October, pp. 954–978, 2021, doi: 10.1016/j.solener.2021.10.070.

[6] X. Shi, Y. Wu, J. Chen, M., Cai, Y. Yang, X. Liu, Y. Tao, M. Guli, Y. Ding, and S. Dai, "Thermally stable perovskite solar cells with efficiency over 21% Via a bifunctional additive," *J. Mater. Chem. A*, vol. 8, no. 15, pp. 7205–7213, 2020, doi: 10.1039/d0ta01255f.

[7] Y. Zhou, J. Hu, Y. Wu, R. Qing, C. Zhang, X. Xu, and M. Jiang ., "Review on methods for improving the thermal and ambient stability of perovskite solar cells," *J. Photonics Energy*, vol. 9, no. 04, p. 1, 2019, doi: 10.1117/1.jpe.9.040901.

[8] R. Xia, Z. Fei, N. Drigo, F.D. Bobbink, Z. Huang, R. Jasiūnas, M. Franckevičius, V. Gulbinas, M. Mensi, X. Fang, and C. Roldán‐Carmona, "Retarding Thermal Degradation in Hybrid Perovskites by Ionic Liquid Additives," *Adv. Funct. Mater.*, vol. 29, no. 22, 2019, doi: 10.1002/adfm.201902021.

[9] Z. Wang, Z. Shi, T. Li, Y. Chen, and W. Huang, "Stability of Perovskite Solar Cells: A Prospective on the Substitution of the A Cation and X Anion," *Angew. Chemie - Int. Ed.*, vol. 56, no. 5, pp. 1190–1212, 2017, doi: 10.1002/anie.201603694.

[10] S. A. U. Hasan, D. S. Lee, S. H. Im, and K. H. Hong, "Present Status and Research Prospects of Tin-based Perovskite Solar Cells," *Sol. RRL*, vol. 4, no. 2, pp. 1–30, 2020, doi: 10.1002/solr.201900310.

[11] M.T. Mbumba, D.M. Malouangou, J.M. Tsiba, M.W. Akram, L. Bai, Y. Yang, and M. Guli, "Compositional engineering solutions for decreasing trap state density and improving thermal stability in perovskite solar cells," *J. Mater. Chem. C*, vol. 9, no. 40, pp. 14047–14064, 2021, doi: 10.1039/d1tc02315b.

[12] Y. Fu, M.P. Hautzinger, Z. Luo, F. Wang, D. Pan, M.M. Aristov, I.A. Guzei, A. Pan, X. Zhu, and S. Jin, "Incorporating Large A Cations into Lead Iodide Perovskite Cages: Relaxed Goldschmidt Tolerance Factor and Impact on Exciton-Phonon Interaction," *ACS Cent. Sci.*, vol. 5, no. 8, pp. 1377–1386, 2019, doi: 10.1021/acscentsci.9b00367.

[13] S. J. Adjogri and E. L. Meyer, "A Review on Lead-Free Hybrid Halide Perovskites as Light Absorbers for Photovoltaic Applications Based on Their Structural, Optical, and Morphological Properties," *Molecules*, vol. 25, no. 21, 2020, doi: 10.3390/molecules25215039.

[14] M.G. Ju, M. Chen, Y. Zhou, J. Dai, L. Ma, N.P. Padture, and X.C. Zeng, "Toward Eco-friendly and Stable Perovskite Materials for Photovoltaics," *Joule*, vol. 2, no. 7, pp. 1231–1241, 2018, doi: 10.1016/j.joule.2018.04.026.

[15] M. Ghasemi, H. Hu, Z. Peng, J.J. Rech, I. Angunawela, J.H. Carpenter, S.J. Stuard, A. Wadsworth, I. McCulloch, W. You, and H. Ade, "Delineation of Thermodynamic and Kinetic Factors that Control Stability in Non-fullerene Organic Solar Cells," *Joule*, vol. 3, no. 5, pp. 1328–1348, 2019, doi: 10.1016/j.joule.2019.03.020.

[16] S. Kundu and T. L. Kelly, "In situ studies of the degradation mechanisms of perovskite solar cells," *EcoMat*, vol. 2, no. 2, pp. 1–22, 2020, doi: 10.1002/eom2.12025.

[17] K. Jaeun, R. Matheus, P. ; Siva, Y. Hasnain, E.-C. Cho;, and Y. Junsin, "A Review of the Degradation of Photovoltaic Modules for Life Expectancy," *J. Palliat. Med.*, vol. 19, no. 4, p. 468, 2016, doi: 10.1089/jpm.2015.0452.

DOI: 10.31695/IJASRE.2023.9.7.1

[18] Z. Shi and A. H. Jayatissa, "Perovskites-based solar cells: A review of recent progress, materials and processing methods," *Materials (Basel).*, vol. 11, no. 5, 2018, doi: 10.3390/ma11050729.

[19] F. Hao, C. C. Stoumpos, R. P. H. Chang, and M. G. Kanatzidis, "Anomalous band gap behavior in mixed Sn and Pb perovskites enables broadening of absorption spectrum in solar cells," *J. Am. Chem. Soc.*, vol. 136, no. 22, pp. 8094–8099, 2014, doi: 10.1021/ja5033259.

[20] A. Bonadio, C.A. Escanhoela, F.P. Sabino, G. Sombrio, V.G. De Paula, F.F. Ferreira, A. Janotti, G.M. Dalpian, and J.A. Souza, "Entropy-driven stabilization of the cubic phase of $MaPbI_3$ at room temperature," *J. Mater. Chem. A*, no. 207890, p. 121, 2014, doi: 10.1039/D0TA10492B.Volume.

[21] Y. Chen, Z. Yang, S. Wang, X. Zheng, Y. Wu, N. Yuan, W.H. Zhang, and S. Liu, "Design of an Inorganic Mesoporous Hole-Transporting Layer for Highly Efficient and Stable Inverted Perovskite Solar Cells," *Adv. Mater.*, vol. 30, no. 52, pp. 1–9, 2018, doi: 10.1002/adma.201805660.

[22] C. C. Boyd, R. Cheacharoen, T. Leijtens, and M. D. McGehee, "Understanding Degradation Mechanisms and Improving Stability of Perovskite Photovoltaics," *Chem. Rev.*, vol. 119, no. 5, pp. 3418–3451, 2019, doi: 10.1021/acs.chemrev.8b00336.

[23] S. Seo, S. Jeong, C. Bae, N.-G. Park, and H. Shin, "Perovskite Solar Cells: Perovskite Solar Cells with Inorganic Electron- and Hole-Transport Layers Exhibiting Long-Term (≈500 h) Stability at 85 ° C under Continuous 1 Sun Illumination in Ambient Air (Adv. Mater. 29/2018)," *Adv. Mater.*, vol. 30, no. 29, p. 1870210, 2018, doi: 10.1002/adma.201870210.

[24] R. Wang, M. Mujahid, Y. Duan, Z. K. Wang, J. Xue, and Y. Yang, "A Review of Perovskites Solar Cell Stability," *Adv. Funct. Mater.*, vol. 29, no. 47, pp. 1–25, 2019, doi: 10.1002/adfm.201808843.

[25] N. Van Toan, T. T. K. Tuoi, N. Inomata, M. Toda, and T. Ono, "Aluminum doped zinc oxide deposited by atomic layer deposition and its applications to micro/nano devices," *Sci. Rep.*, vol. 11, no. 1, pp. 1–12, 2021, doi: 10.1038/s41598-020-80880-3.

[26] Y. Wu, X. Yang, W. Chen, Y. Yue, M. Cai, F. Xie, E. Bi, A. Islam, and L. Han, "Perovskite solar cells with 18.21% efficiency and area over 1 cm^2 fabricated by heterojunction engineering," *Nat. Energy*, vol. 1, no. 11, 2016, doi: 10.1038/nenergy.2016.148.

[27] S. Abicho, B. Hailegnaw, G. A. Workneh, and T. Yohannes, "Role of additives and surface passivation on the performance of perovskite solar cells," *Mater. Renew. Sustain. Energy*, vol. 11, no. 1, pp. 47–70, 2022, doi: 10.1007/s40243-021-00206-9.

[28] R. Zheng, S. Zhao, H. Zhang, H. Li, J. Zhuang, X. Liu, H. Li, and H. Wang, "Defect passivation grain boundaries using 3-aminopropyltrimethoxysilane for highly efficient and stable perovskite solar cells," *Sol. Energy*, vol. 224, no. December 2020, pp. 472–479, 2021, doi: 10.1016/j.solener.2021.06.001.

[29] R. M. I. Bandara, S. M. Silva, C. C. L. Underwood, K. D. G. I. Jayawardena, R. A. Sporea, and S. R. P. Silva, "Progress of Pb-Sn Mixed Perovskites for Photovoltaics: A Review," *Energy Environ. Mater.*, vol. 5, no. 2, pp. 370–400, 2022, doi: 10.1002/eem2.12211.

[30] T. Leijtens, K. Bush, R. Cheacharoen, R. Beal, A. Bowring, and M. D. McGehee, "Towards enabling stable lead halide perovskite solar cells; Interplay between structural, environmental, and thermal stability," *J. Mater. Chem. A*, vol. 5, no. 23, pp. 11483–11500, 2017, doi: 10.1039/c7ta00434f.

[31] F. Wang, J. Ma, F. Xie, L. Li, J. Chen, J. Fan, and N. Zhao, "Organic Cation - Dependent Degradation Mechanism of Organotin Halide Perovskites," *Adv. Funct. Mater.*, vol. 26, no. 20, pp. 3417–3423, 2016, doi: https://doi.org/10.1002/adfm.201505127.

[32] M. Li, R. Sun, J. Chang, J. Dong, Q. Tian, H. Wang, Z. Li, P. Yang, H. Shi, C. Yang, and Z. Wu, "Orientated crystallization of FA-based perovskite via hydrogen-bonded polymer network for efficient and stable solar cells," *Nat. Commun.*, vol. 14, no. 1, pp. 1–11, 2023, doi: 10.1038/s41467-023-36224-6.

[33] S. Lv, W. Gao, Y. Liu, H. Dong, N. Sun, T. Niu, Y. Xia, Z. Wu, L. Song, C. Ran, and L. Fu, "Stability of Sn-Pb mixed organic–inorganic halide perovskite solar cells: Progress, challenges, and perspectives," *J. Energy Chem.*, vol. 65, pp. 371–404, 2021, doi: 10.1016/j.jechem.2021.06.011.

[34] X. Diao, Y. Tang, D. Xiong, P. Wang, and L. Gao, "Study on the properties of perovskite materials under light and different temperatures and electric fields based on DFT," *R. Soc. Chem.*, pp. 20960–20971, 2020, doi: 10.1039/d0ra02841j.

[35] M. Lhouceine, B. Omar, N. Abdelhafid, and R. Khalid, "The study of electronic and optical properties of perovskites $CH_3NH_3PbCl_3$ and $CH_3NH_3PbBr_3$ using first-principle," *E3S Web Conf. 336, 00015*, no. January, 2022, doi: 10.1051/e3sconf/202233600015.

[36] K. Korshunova, L. Winterfeld, W. J. D. Beenken, and E. Runge, "Thermodynamic stability of mixed Pb:Sn methyl-ammonium halide perovskites," *Phys. Status Solidi Basic Res.*, vol. 253, no. 10, pp. 1907–1915, 2016, doi: 10.1002/pssb.201600136.

[37] C.M.M. Soe, G.P. Nagabhushana, R. Shivaramaiah, H. Tsai, W. Nie, J.C. Blancon, F. Melkonyan, D.H. Cao, B. Traoré, L. Pedesseau, and M. Kepenekian, "Structural and thermodynamic limits of layer thickness in 2D halide perovskites," *Proc.*

DOI: 10.31695/IJASRE.2023.9.7.1

Natl. Acad. Sci. U. S. A., vol. 116, no. 1, pp. 58–66, 2019, doi: 10.1073/pnas.1811006115.

[38] W. Travis, E. N. K. Glover, H. Bronstein, D. O. Scanlon, and R. G. Palgrave, "On the application of the tolerance factor to inorganic and hybrid halide perovskites: A revised system," *Chem. Sci.*, vol. 7, no. 7, pp. 4548–4556, 2016, doi: 10.1039/c5sc04845a.

[39] C. C. Stoumpos, C. D. Malliakas, and M. G. Kanatzidis, "Semiconducting tin and lead iodide perovskites with organic cations: Phase transitions, high mobilities, and near-infrared photoluminescent properties," *Inorg. Chem.*, vol. 52, no. 15, pp. 9019–9038, 2013, doi: 10.1021/ic401215x.

[40] T. Baikie, Y. Fang, J.M. Kadro, M. Schreyer, F. Wei, S.G. Mhaisalkar, M. Graetzel, and T.J. White, "Synthesis and crystal chemistry of the hybrid perovskite $(CH_3NH_3)PbI_3$ for solid-state sensitised solar cell applications," *J. Mater. Chem. A*, vol. 1, no. 18, pp. 5628–5641, 2013, doi: 10.1039/c3ta10518k.

[41] Q. Liu, A. Li, W. Chu, O. V. Prezhdo, and W. Z. Liang, "Influence of intrinsic defects on the structure and dynamics of the mixed Pb-Sn perovskite: first-principles DFT and NAMD simulations," *J. Mater. Chem. A*, vol. 10, no. 1, pp. 234–244, 2022, doi: 10.1039/d1ta09027e.

[42] J. Huang, Y. Yuan, Y. Shao, and Y. Yan, "Understanding the physical properties of hybrid perovskites for photovoltaic applications," *Nat. Rev. Mater.*, vol. 2, 2017, doi: 10.1038/natrevmats.2017.42.

[43] J. Enkovaara, C. Rostgaard, and J. J. Mortensen, "Advanced capabilities for materials modelling with Quantum ESPRESSO," *J. Phys.*, vol. 29, 2017, doi: https://doi.org/10.1088/1361-648X/aa8f79.

[44] M. I. Kholil, M. T. H. Bhuiyan, M. A. Rahman, M. S. Ali, and M. Aftabuzzaman, "Effects of Fe doping on the visible light absorption and bandgap tuning of lead-free ($CsSnCl_3$) and lead halide ($CsPbCl_3$) perovskites for optoelectronic applications," *AIP Adv.*, vol. 11, no. 3, 2021, doi: 10.1063/5.0042847.

[45] A. Rajagopal, Z. Yang, S.B. Jo, I.L. Braly, P.W. Liang, H.W. Hillhouse, and A.K.Y. Jen, "Highly Efficient Perovskite-Perovskite Tandem Solar Cells Reaching 80% of the Theoretical Limit in Photovoltage," *Adv. Mater.*, vol. 28, no. 40, pp. 8990–8997, 2016, doi: 10.1002/adma.201602696.

[46] X. Liu, Z. Yang, C. Chueh, and A. Rajagopal, "Improved efficiency and stability of Pb–Sn binary perovskite solar cells by Cs substitution," *J. Mater. Chem. A Mater. energy Sustain.*, vol. 4, pp. 17939–17945, 2016, doi: 10.1039/C6TA07712A.

[47] A. Johnson, F. Gbaorun, and B.A. Ikyo, "First - principles study of (CsMA) $NaSbX_6$ (MA = methylammonium ; X = Cl , Br , I) organic – inorganic hybrid double perovskites for optoelectronic applications," *J. Comput. Electron.*, vol. 21, no. 1, pp. 34–39, 2022, doi: 10.1007/s10825-021-01832-2.

[48] M. S. Tumusange, B. Subedi, C. Chen, M. M. Junda, Z. Song, and N. J. Podraza, "Impact of Humidity and Temperature on the Stability of the Optical Properties and Structure of $MAPbI_3$, $MA_{0.7}FA_{0.3}PbI_3$ and $(FAPbI_3)_{0.95}(MAPbBr_3)_{0.05}$ Perovskite Thin Films," *Materials (Basel).*, vol. 95, 2021.

[49] H. M. Ghaithan, Z. A. Alahmed, S. M. H. Qaid, and A. S. Aldwayyan, "Density Functional Theory Analysis of Structural, Electronic, and Optical Properties of Mixed-Halide Orthorhombic Inorganic Perovskites," *ACS Omega*, vol. 6, no. 45, pp. 30752–30761, 2021, doi: 10.1021/acsomega.1c04806.

[50] M. Pazoki, T.J. Jacobsson, S.H. Cruz, M.B. Johansson, R. Imani, J. Kullgren, A. Hagfeldt, E.M. Johansson, T. Edvinsson, and G. Boschloo, "Photon Energy-Dependent Hysteresis Effects in Lead Halide Perovskite Materials," *J. Phys. Chem. C*, vol. 121, no. 47, pp. 26180–26187, 2017, doi: 10.1021/acs.jpcc.7b06775.

[51] K. K. Ostrikov, H. Wang, and A. Du, "Towards lead-free perovskite photovoltaics and optoelectronics by ab-initio simulations," *Sci. Rep.*, vol. 7, no. 1, pp. 1–9, 2017, doi: 10.1038/s41598-017-13172-y.

[52] S. Mazumdar, Y. Zhao, and X. Zhang, "Stability of Perovskite Solar Cells : Degradation Mechanisms and Remedies," vol. 2, no. August, pp. 1–34, 2021, doi: 10.3389/felec.2021.712785.

[53] M. Ha, A. Karmakar, G.M. Bernard, E. Basilio, A. Krishnamurthy, A.M. Askar, K. Shankar, S. Kroeker, and V.K. Michaelis, "Phase Evolution in Methylaamonium Tin Halide Perovskites with Variable Temperature Solid-State Sn NMR Spectroscopy," *J. Phys. Chem. C*, 2020, doi: 10.1021/acs.jpcc.0c03589.

[54] K. J. Savill, A. M. Ulatowski, and L. M. Herz, "Optoelectronic Properties of Tin − Lead Halide Perovskites," *ACS Energy Lett.*, vol. 6, p. 2413−2426, 2021, doi: 10.1021/acsenergylett.1c00776.

[55] H. Liu, X. Li, Y. Zeng, and L. Meng, "Effects of halogen substitutions on the properties of $CH_3NH_3Sn_{0.5}Pb_{0.5}I_3$ perovskites," *Comput. Mater. Sci.*, vol. 177, no. January, p. 109576, 2020, doi: 10.1016/j.commatsci.2020.109576.

[56] S. Zhu, J. Ye, Y. Zhao, and Y. Qiu, "Structural, Electronic, Stability, and Optical Properties of $CsPb_{1-x}Sn_xIBr_2$ Perovskites: A First-Principles Investigation," *J. Phys. Chem. C*, vol. 123, no. 33, pp. 20476–20487, 2019, doi: 10.1021/acs.jpcc.9b04841.

[57] S. Ašmontas and A. Cerškus, "Impact of Cesium Concentration on Optoelectronic Properties of Metal Halide Perovskites," *Materials (Basel).*, vol. 15, no. 5, p. 1936, 2022, doi: https://doi.org/10.3390/ma15051936.

[58] G. Niu, W. Li, J. Li, X. Liang, and L. Wang, "Enhancement of thermal stability for perovskite solar cells through cesium doping," *RSC Adv.*, vol. 7, no. 28, pp. 17473–17479, 2017, doi: 10.1039/c6ra28501e.

[59] Q. ou, S. Gu, and X. Gou, "The Highly Accurate Interatomic Potential of $CsPbBr_3$ Perovskite with Temperature

DOI: 10.31695/IJASRE.2023.9.7.1

Dependence on the Structure and Thermal Properties," *Materials (Basel).*, vol. 16, no. 5, p. 2043, 2023.

[60] A. Ciccioli and A. Latini, "Thermodynamics and the Intrinsic Stability of Lead Halide Perovskites $CH_3NH_3PbX_3$," *J. Phys. Chem. Lett.*, vol. 9, no. 13, pp. 3756–3765, 2018, doi: 10.1021/acs.jpclett.8b00463.

*Corresponding author: mtmbumba@gmail.com

DOI: 10.31695/IJASRE.2023.9.7.1